

Symmetry enriched U(1) topological orders for dipole-octupole doublets on a pyrochlore lattice

Yao-Dong Li¹ and Gang Chen^{1,2,*}¹State Key Laboratory of Surface Physics, Center for Field Theory and Particle Physics, Department of Physics, Fudan University, Shanghai 200433, People's Republic of China²Collaborative Innovation Center of Advanced Microstructures, Nanjing, 210093, People's Republic of China (Received 22 September 2016; revised manuscript received 25 December 2016; published 19 January 2017)

Symmetry plays a fundamental role in our understanding of both conventional symmetry breaking phases and the more exotic quantum and topological phases of matter. We explore the experimental signatures of symmetry enriched U(1) quantum spin liquids (QSLs) on the pyrochlore lattice. We point out that the Ce local moment of the newly discovered pyrochlore QSL candidate $\text{Ce}_2\text{Sn}_2\text{O}_7$, is a dipole-octupole doublet. The generic model for these unusual doublets supports two distinct symmetry enriched U(1) QSL ground states in the corresponding quantum spin ice regimes. These two U(1) QSLs are dubbed dipolar U(1) QSL and octupolar U(1) QSL. While the dipolar U(1) QSL has been discussed in many contexts, the octupolar U(1) QSL is rather unique. Based on the symmetry properties of the dipole-octupole doublets, we predict the peculiar physical properties of the octupolar U(1) QSL, elucidating the unique spectroscopic properties in the external magnetic fields. We further predict the Anderson-Higgs transition from the octupolar U(1) QSL driven by the external magnetic fields. We identify the experimental relevance with the candidate material $\text{Ce}_2\text{Sn}_2\text{O}_7$ and other dipole-octupole doublet systems.

DOI: 10.1103/PhysRevB.95.041106

Introduction. The interplay between symmetry and topology is the frontier subject in modern condensed matter physics [1–3]. At the single particle level, the nontrivial realization of time reversal symmetry in electron band structure has led to the discovery of topological insulators [4,5]. For the intrinsic topological order such as Z_2 toric code and chiral Abelian topological order, a given symmetry of the system could enrich the topological order into distinct phases that cannot be smoothly connected without crossing a phase transition [6–9]. Despite the active theoretical efforts, the experimentally relevant symmetry enriched topological order is extremely rare. In this Rapid Communication, we explore one physical realization of *symmetry enriched U(1) topological order* for the dipole-octupole (DO) doublets on the pyrochlore lattice and predict the experimental consequences of distinct symmetry enrichment. The DO doublet is a special Kramers' doublet in the D_{3d} crystal field environment [10–12]. Both states of the DO doublet transform as the one-dimensional irreducible representations (Γ_5^+ or Γ_6^+) of the D_{3d} point group [10]. It was realized that the DO doublets on the pyrochlore lattice could support two distinct U(1) quantum spin liquid (QSL) ground states [10]. These distinct U(1) QSLs are the symmetry enriched U(1) topological orders [13] and are enriched by the lattice symmetries of the pyrochlore systems.

Recently $\text{Ce}_2\text{Sn}_2\text{O}_7$ was proposed as the first Ce-based QSL candidate in the pyrochlore family [14], in which no magnetic order was observed down to 0.02 K. Although it was not noticed previously, the Ce^{3+} local moment in $\text{Ce}_2\text{Sn}_2\text{O}_7$ is actually a DO doublet. The strong atomic spin-orbit coupling (SOC) of the $4f^1$ electron in the Ce^{3+} ion entangles the electron spin ($S = 1/2$) with the orbital angular momentum ($L = 3$) into a $J = 5/2$ total moment. The sixfold degeneracy of the $J = 5/2$ total moment is further split into three Kramers' doublets by the D_{3d} crystal field (see Fig. 1). Since the ground

state doublet wave functions are combinations of $J^z = \pm 3/2$ states [14], this doublet is precisely the DO doublet that we defined [10]. Because the crystal field gap is much larger than the interaction energy scale of the local moments and the temperature scale in the experiments, the low temperature magnetic property of $\text{Ce}_2\text{Sn}_2\text{O}_7$ is fully governed by the ground state doublets.

Motivated by the experiments on $\text{Ce}_2\text{Sn}_2\text{O}_7$ and more generally by the experimental consequences of the distinct symmetry enriched U(1) QSLs for the DO doublets, in this Rapid Communication, we explore the peculiar properties of the DO doublets in external magnetic fields. In the octupolar U(1) QSL of the octupolar quantum spin ice regime for the DO doublets, we find that the external magnetic field directly couples to the spinons and modifies the spinon dispersions. This effect allows us to control the spinon excitations with the magnetic fields. The lower excitation edge of the spinon continuum in the dynamic spin structure factors can thus be modified by the magnetic fields, which gives a sharp prediction for the inelastic neutron scattering experiments. When the magnetic field exceeds the critical value and closes the spinon gap, the spinons are condensed, driving the system through

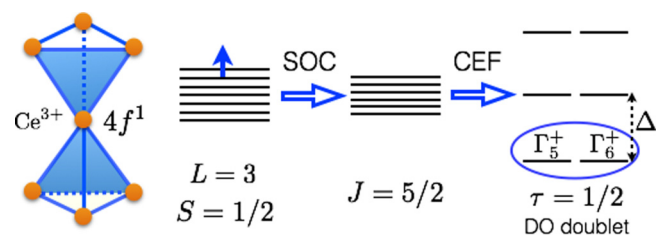


FIG. 1. The electron configuration and the D_{3d} crystal electric field (CEF) splitting of the Ce^{3+} ion in $\text{Ce}_2\text{Sn}_2\text{O}_7$. The CEF ground state wave functions are combinations of $J^z = \pm 3/2$ states [14], thus the CEF ground state is a DO doublet. Δ is the CEF gap and was fitted to be $\Delta = 50 \pm 5$ meV [14].

*gangchen.physics@gmail.com

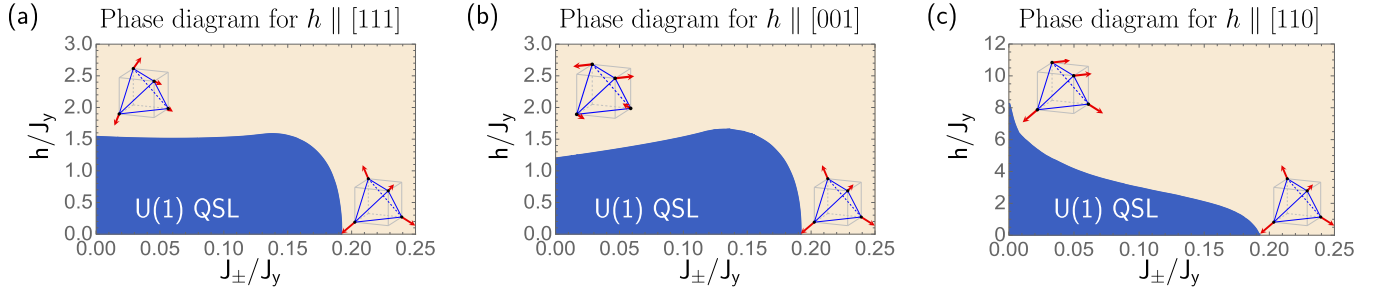


FIG. 2. Phase diagrams for magnetic fields along (a) [111], (b) [001], and (c) [110] directions. Outside the QSL phases are the induced magnetic ordered phase via the spinon condensation. For $h = 0$, the spinons are condensed at $\mathbf{k}_c = (0,0,0)$, and we choose the local moments to order in the local \hat{z} direction. In (a), a large magnetic field near the vertical axis drives the spinon condensation at $\mathbf{k}_c = \pi(1,1,1)$, and the resulting order is depicted in the figure. This order smoothly connects to the order on the horizontal axis. The cases in (b) and (c) are similar, except that in (b) the field on the vertical axis drives the condensation at $\mathbf{k}_c = 2\pi(0,0,1)$, while in (c) $\mathbf{k}_c = \pi(1,1,0)$ near the vertical axis. We set the diamond lattice constant to unity.

an Anderson-Higgs' transition and inducing the long-range magnetic orders.

Generic model for DO doublets on the pyrochlore lattice. Because of the peculiar symmetry properties of the DO doublets, the most generic model that describes the nearest-neighbor interaction between them is given as $H_{\text{DO}} = \sum_{\langle ij \rangle} [J_x \tau_i^x \tau_j^x + J_y \tau_i^y \tau_j^y + J_z \tau_i^z \tau_j^z + J_{xz} (\tau_i^x \tau_j^z + \tau_i^z \tau_j^x)]$ [10]. Here the interaction is uniform on every bond despite the fact that the DO doublet involves a significant contribution from the orbital part due to the strong SOC [15–20], and the DO doublet is modeled by an effective pseudospin-1/2 moment τ . Both τ^x and τ^z transform as the dipole moments under the space group symmetry, while the τ^y component behaves as an octupole moment [10]. It is this important difference that leads to some of the unique properties of its U(1) QSL ground states.

Due to the spatial uniformity of the generic model, we can transform the model H_{DO} into the XYZ model with

$$H_{\text{XYZ}} = \sum_{\langle ij \rangle} \tilde{J}_x \tilde{\tau}_i^x \tilde{\tau}_j^x + \tilde{J}_y \tilde{\tau}_i^y \tilde{\tau}_j^y + \tilde{J}_z \tilde{\tau}_i^z \tilde{\tau}_j^z, \quad (1)$$

where $\tilde{\tau}^x$ and $\tilde{\tau}^z$ (\tilde{J}_x and \tilde{J}_z) are related to τ^x and τ^z (J_x and J_z) by a rotation around the y direction in the pseudospin space, and $\tilde{\tau}^y \equiv \tau^y$, $\tilde{J}_y \equiv J_y$. When one of the couplings, \tilde{J}_μ , is dominant and antiferromagnetic, the corresponding pseudospin component, $\tilde{\tau}^\mu$, is regarded as the Ising component of the model, and the ground state is a U(1) QSL in the corresponding quantum spin ice regime. The dipolar U(1) QSL is realized when the Ising component is the dipole moment $\tilde{\tau}^x$ or $\tilde{\tau}^z$, while the octupolar U(1) QSL is realized when the Ising component is the octupole moment $\tilde{\tau}^y$. In the compact U(1) quantum electrodynamics description of the low energy properties of the U(1) QSL [21,22], the Ising component is identified as the emergent electric field [21]. Therefore, the emergent electric field transforms very differently under the lattice symmetry in dipolar and octupolar U(1) QSLs, making these two U(1) QSLs symmetry enriched U(1) topological order on the pyrochlore lattice [10].

Octupolar U(1) QSL and field-driven Anderson-Higgs' transitions. Since the dipolar U(1) QSL has been discussed many times in literature [10,23–31], we here focus on the octupolar U(1) QSL of the octupolar quantum spin ice regime

where \tilde{J}_y is dominant and antiferromagnetic. The octupolar U(1) QSL is a new phase that is *unique* to the DO doublet and cannot be found in any other doublets on the pyrochlore lattice.

We consider the coupling of the DO doublet to the external magnetic field. Remarkably, because $\tilde{\tau}^y$ is an octupole moment, it does not couple to the magnetic field even though it is time reversally odd. Only the dipolar component τ^z couples linearly to the external magnetic field. The resulting model is

$$H = \sum_{\langle ij \rangle} \sum_{\mu=x,y,z} \tilde{J}_\mu \tilde{\tau}_i^\mu \tilde{\tau}_j^\mu - \sum_i h (\hat{n} \cdot \hat{z}_i) \tau_i^z, \quad (2)$$

where \hat{n} is the direction of the magnetic field and \hat{z}_i is the z direction of the local coordinate basis at the lattice site i [32]. This generic model describes *all* magnetic properties of the DO doublets on the pyrochlore lattice.

As the generic model contains four parameters, it necessarily brings some unnecessary complication into the problem. To capture the essential physics, we here consider a simplified version of the generic model in Eq. (2). The simplified model is

$$H_{\text{sim}} = \sum_{\langle ij \rangle} J_y \tau_i^y \tau_j^y - J_\pm (\tau_i^+ \tau_j^- + \text{H.c.}) - \sum_i h (\hat{n} \cdot \hat{z}_i) \tau_i^z, \quad (3)$$

where we define $\tau_i^\pm = \tau_i^z \pm i \tau_i^x$ and \hat{n} is the direction of the external magnetic field. In the Ising limit with $J_\pm = 0$ and $h = 0$, the antiferromagnetic J_y favors the τ^y components to be in the ice manifold and requires a “two-plus two-minus” ice constraint for the τ^y configuration on each tetrahedron. This octupolar ice manifold is extensively degenerate. With a small and finite J_\pm or h , the system can then tunnel quantum mechanically within the octupolar ice manifold and form an octupolar U(1) QSL. In this perturbative limit, the degenerate perturbation theory yields an effective ring exchange model with [32]

$$H_{\text{ring}} = J_{\text{ring}} \sum_{\square} [\tau_i^+ \tau_j^- \tau_k^+ \tau_l^- \tau_m^+ \tau_n^- + \text{H.c.}], \quad (4)$$

where “ i, j, k, l, m, n ” are six sites on the perimeter of the elementary hexagon of the pyrochlore lattice, and the ring

exchange $J_{\text{ring}} < 0$ for $J_{\pm} > 0$ and for either sign of h . H_{ring} does not involve defect tetrahedra that violate the ice constraint and thus only describes the quantum fluctuation and dynamics *within* the ice manifold. It is well known that the low energy properties of H_{ring} are described by the compact U(1) quantum electrodynamics [21] of the U(1) QSL with gapless gauge photon, and the spin-flip operator τ_i^{\pm} is identified as the gauge string within the ice manifold. We expect the simplified model H_{sim} captures the generic properties of the octupolar U(1) QSL.

To obtain the phase diagram of H_{sim} , we start from the octupolar U(1) QSL phase and study its instability. For this purpose, we include the spinon excitations (that are out of the ice manifold) into the formulation. The perturbative analysis and H_{ring} , that focus on the ice manifold, do not capture the spinons. We here implement a parton-gauge construction for the octupolar U(1) QSL and formulate H_{sim} into a lattice gauge theory with the spinons. Like many other parton construction, we replace the physical Hilbert space with a larger one and supplement it with a constraint. We follow Refs. [23,24] and express the pseudospin operators as

$$\tau_i^+ = \Phi_{\mathbf{r}}^{\dagger} \Phi_{\mathbf{r}'} s_{\mathbf{r}\mathbf{r}'}^+, \quad \tau_i^- = s_{\mathbf{r}\mathbf{r}'}^-, \quad (5)$$

where $\mathbf{r}\mathbf{r}'$ is the link that connects two neighboring tetrahedral centers at \mathbf{r} and \mathbf{r}' , and the pyrochlore site i is shared by the two tetrahedra. The centers of the tetrahedra form a diamond lattice, and \mathbf{r} (\mathbf{r}') belongs to the I (II) diamond sublattice. Here $s_{\mathbf{r}\mathbf{r}'}$ is a spin-1/2 variable that corresponds to the emergent gauge field, and $\Phi_{\mathbf{r}}^{\dagger}$ ($\Phi_{\mathbf{r}}$) creates (annihilates) one spinon at the diamond site \mathbf{r} . The spinons carry the emergent electric charge, and $\Phi_{\mathbf{r}}^{\dagger}$ and $\Phi_{\mathbf{r}}$ are raising and lowering operators of the emergent electric charge. Since we enlarged the physical Hilbert space, the constraint $Q_{\mathbf{r}} = \eta_{\mathbf{r}} \sum_{\mu} \tau_{\mathbf{r},\mathbf{r}+\eta_{\mathbf{r}}\mathbf{e}_{\mu}}^y$ is imposed, where $\eta_{\mathbf{r}} = 1$ (-1) for the I (II) sublattice and the \mathbf{e}_{μ} 's are the first neighbor vectors of the diamond lattice. Here $Q_{\mathbf{r}}$ measures the electric charge at \mathbf{r} and satisfies

$$[\Phi_{\mathbf{r}}, Q_{\mathbf{r}}] = \Phi_{\mathbf{r}}, \quad [\Phi_{\mathbf{r}}^{\dagger}, Q_{\mathbf{r}}] = -\Phi_{\mathbf{r}}^{\dagger}. \quad (6)$$

The U(1) QSL of quantum spin ice is an example of the string-net condensed phases [34]. In the U(1) QSL, τ_i^{\pm} creates the shortest open (gauge) string whose ends are spinon particles. In the spin ice context, τ_i^{\pm} creates two defect tetrahedra that violate the ‘‘two-plus two-minus’’ ice constraint. The parton-gauge construction captures this essential property, and the model becomes

$$H_{\text{sim}} = \sum_{\mathbf{r}} \frac{J_y Q_{\mathbf{r}}^2}{2} - \sum_{\mathbf{r}} \sum_{\mu \neq \nu} J_{\pm} \Phi_{\mathbf{r}+\eta_{\mathbf{r}}\mathbf{e}_{\mu}}^{\dagger} \Phi_{\mathbf{r}+\eta_{\mathbf{r}}\mathbf{e}_{\nu}} s_{\mathbf{r},\mathbf{r}+\eta_{\mathbf{r}}\mathbf{e}_{\mu}}^{-\eta_{\mathbf{r}}} \times s_{\mathbf{r},\mathbf{r}+\eta_{\mathbf{r}}\mathbf{e}_{\nu}}^{+\eta_{\mathbf{r}}} - \sum_{(\mathbf{r}\mathbf{r}')} \frac{h}{2} (\hat{n} \cdot \hat{z}_i) (\Phi_{\mathbf{r}}^{\dagger} \Phi_{\mathbf{r}'} s_{\mathbf{r}\mathbf{r}'}^+ + \text{H.c.}) \quad (7)$$

With the constraint, Eq. (7) is an exact reformulation of the simplified model in Eq. (3). It describes the bosonic spinons hopping on the diamond lattice. The spinons are minimally coupled with the emergent U(1) gauge field. Remarkably, the external magnetic field directly couples to the spinons and does *not* couple to the emergent electric field. This is sharply distinct from the dipolar U(1) QSL where the magnetic field would also directly couple with the emergent electric field.

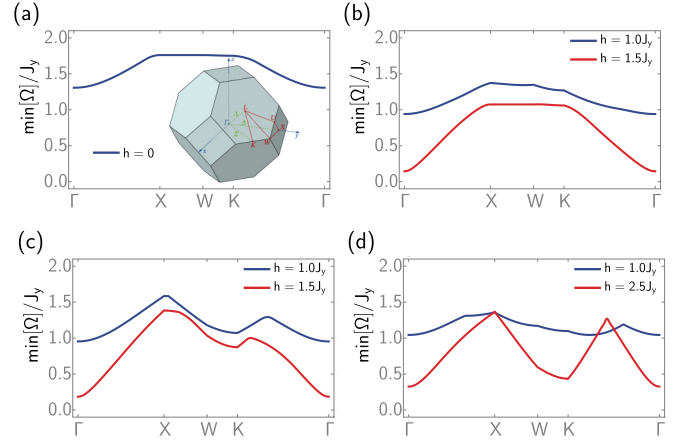


FIG. 3. Lower excitation edges of the spinon continuum in the dynamic spin structure factor under (a) zero magnetic field, and field along (b) [111], (c) [001], and (d) [110] directions. In the figure, we set $J_{\pm} = 0.1 J_y$. The inset of (a) is the Brillouin zone [33].

Inside the U(1) QSL, the spinons are fully gapped. The external magnetic field allows the spinon to tunnel between the neighbor tetrahedra that are located along the field direction. As we increase the magnetic field h , the spinon gap gradually decreases. It is expected that, at a critical field strength, the spinon gap is closed and the spinons are condensed with $\langle \Phi_{\mathbf{r}} \rangle \neq 0$. Via the Anderson-Higgs’ mechanism, the U(1) gauge field becomes massive and gapped. Note that this differs from the Coulomb ferromagnet where the gauge field remains gapless and deconfined [23]. The resulting proximate state develops a long-range magnetic order. Therefore, this is an Anderson-Higgs’ transition driven by the external magnetic fields. This is a generic property of the octupolar U(1) QSL and is not a specific property of the simplified model. This is an example that an external probe drives an Anderson-Higgs’ transition in a physical system.

To solve the reformulated model in Eq. (7), we adopt the gauge mean-field approximation [10,23–25]. In this approximation, we decouple the model into the spinon sector and the gauge sector. Since H_{ring} favors a zero background gauge flux on each elementary hexagon of the diamond lattice, we solve for the mean-field ground state within this sector [32]. The magnetic dipolar order is obtained by evaluating

$$\langle \tau_i^z \rangle = \frac{1}{2} [\langle \tau_i^+ \rangle + \langle \tau_i^- \rangle] \quad (8)$$

$$= \frac{1}{2} [\langle \Phi_{\mathbf{r}}^{\dagger} \Phi_{\mathbf{r}'} \rangle \langle s_{\mathbf{r}\mathbf{r}'}^+ \rangle + \text{H.c.}], \quad (9)$$

where $\langle \dots \rangle$ is taken with respect to the ground state. Because of the Zeeman coupling, $\langle \tau_i^z \rangle$ is nonzero even in the U(1) QSL phase where the spinons are not condensed. In the proximate ordered state, the spinon condensate gives an additional contribution that is the induced magnetic order. For all three directions of the external magnetic field, even though the spinons are condensed at finite momenta, the proximate magnetic order preserves the translation symmetry.

The full phase diagrams and the field-induced proximate magnetic orders are depicted in Fig. 2. The magnetic field is found to be least effective in destructing the U(1) QSL for the field along the [110] direction. This is because the

TABLE I. List of the physical properties of different U(1) QSLs on the pyrochlore lattice. “Usual Kramers doublet” refers to the Kramers doublet that is not a DO doublet. They transform as a two-dimensional irreducible representation under the D_{3d} point group. Although the dipolar U(1) QSL for DO doublets behaves the same as the one for usual Kramers’ doublets, their physical origins are rather different [32].

Different U(1) QSLs	Heat capacity	Inelastic neutron scattering measurement
Octupolar U(1) QSL for DO doublets	$C_v \sim T^3$	Gapped spinon continuum
Dipolar U(1) QSL for DO doublets	$C_v \sim T^3$	Both gapless gauge photon and gapped spinon continuum
Dipolar U(1) QSL for non-Kramers’ doublets [24]	$C_v \sim T^3$	Gapless gauge photon
Dipolar U(1) QSL for usual Kramers’ doublets [23]	$C_v \sim T^3$	Both gapless gauge photon and gapped spinon continuum

local \hat{z} direction of two sublattices are orthogonal to the [110] direction, and the pseudospins on them do not couple to the external field. The phase transition is found to be continuous within the gauge mean-field theory and may turn weakly first order after the fluctuations are included. Nevertheless, as the spinon gap is very small near the phase transition, this means that the heat capacity and the magnetic entropy will be more pronounced at low temperatures in these regions.

Lower excitation edges of the dynamic spin structure factors. A smoking gun confirmation of U(1) QSL is to directly measure the gapless U(1) gauge photon and/or the spinon continuum by inelastic neutron scattering (INS) measurement. For the DO doublet, the neutron spin couples to the local moment in the same way as the external magnetic field. Therefore, for the octupolar U(1) QSL, the INS directly probes the spinon excitation, and one would *only* observe the spinon continuum instead of the gapless U(1) gauge photon. The latter was proposed for the dipolar U(1) QSL. This is the sharp difference between the octupolar U(1) QSL and the dipolar U(1) QSL.

In the U(1) QSL, the spinon excitation has two branches due to the two sublattice structure of the diamond lattice. *Specifically* for the simplified model H_{sim} , the two spinon branches are degenerate in the absence of the external magnetic field because the spinons do not hop from one sublattice to another. As shown in Eq. (7), however, the magnetic field allows the spinons to tunnel between the sublattices and breaks the degeneracy of the two spinon bands. The splitted spinon bands are labeled by $\omega_1(\mathbf{k})$ and $\omega_2(\mathbf{k})$ [32].

The INS measures the dynamic spin structure factor $\langle \tau^z \tau^z \rangle_{\mathbf{q}, \Omega}$, where \mathbf{q} and Ω are the neutron momentum and energy transfer, respectively. As τ^z is a spinon bilinear, one neutron spin flip creates one spinon-antispinon pair that shares the neutron energy and momentum transfer. From the conservation of the momentum and the energy, we have

$$\mathbf{q} = \mathbf{k}_1 + \mathbf{k}_2, \quad (10)$$

$$\Omega(\mathbf{q}) = \omega_i(\mathbf{k}_1) + \omega_j(\mathbf{k}_2), \quad (11)$$

where $i, j = 1, 2$ are the band indices, and \mathbf{k}_1 and \mathbf{k}_2 are the momenta of the two spinons.

The lower excitation edge of the dynamic spin structure factor encodes the minimum of the spinon excitation $\Omega(\mathbf{q})$ for each \mathbf{q} . In Fig. 3, we plot the dispersion of the lower spinon excitation edge along the high symmetric momentum direction in the octupolar U(1) QSL for different external field orientations. The field modifies the spinon dispersion and then

tunes the spinon excitation edge. As far as we are aware of, this is a rare example that one can control the spinon excitations in a QSL.

Discussion. Many DO doublet pyrochlores are actually magnetically ordered [35–42], which makes the QSL candidate $\text{Ce}_2\text{Sn}_2\text{O}_7$ rather unique. $\text{Ce}_2\text{Sn}_2\text{O}_7$ has the Curie-Weiss temperature $\Theta_{\text{CW}} \approx -0.25$ K. It was argued in Ref. [14] that an antiferromagnetic Θ_{CW} cannot support a QSL in the spin ice regime. This conclusion is certainly true for the usual Kramers’ doublet but is not the case for the DO doublets. For the DO doublets, what Θ_{CW} measures is J_z , not \tilde{J}_z nor \tilde{J}_x [32]. What determines the phase diagram of H_{XYZ} are \tilde{J}_μ ’s, not the sign or value of the single parameter J_z . One cannot rule out the possibility of the dipolar U(1) QSL in $\text{Ce}_2\text{Sn}_2\text{O}_7$. Moreover, the occurrence of octupolar U(1) QSL as a ground state of H_{XYZ} is actually insensitive to the sign of J_z . If the ground state of $\text{Ce}_2\text{Sn}_2\text{O}_7$ does not belong to any other QSLs, the question then nails down to whether it is a dipolar U(1) QSL or an octupolar U(1) QSL.

In Table I we list the thermodynamic and spectroscopic properties of various U(1) QSLs. Clearly, thermodynamic measurements cannot differentiate them because the low-energy properties are all described by the compact U(1) quantum electrodynamics. The INS measurement, however, is a powerful technique to identify the dipolar U(1) QSL and the octupolar U(1) QSL for the DO doublets. As we wrote in Table I, the INS can observe both spinon continuum and gapless gauge photon for the dipolar U(1) QSL while only gapped spinon continuum can be detected for the octupolar U(1) QSL. We further propose the field driven Anderson-Higgs’ transition and the field-controlled dynamic spin structure factor as the unique signatures of the octupolar U(1) QSL. All these predictions can be useful to identify the nature of the QSL ground state in $\text{Ce}_2\text{Sn}_2\text{O}_7$.

To summarize, we predict a field driven Anderson-Higgs’ transition of the octupolar U(1) QSL for the dipole-octupole doublets on the pyrochlore lattice. Inside the U(1) QSL, the lower excitation edges of the spinon continuum are manipulated by the external magnetic fields. This result provides a detectable experimental consequence in the INS measurements. We expect our work will surely stimulate the experimental studies of $\text{Ce}_2\text{Sn}_2\text{O}_7$ and other pyrochlore systems with dipole-octupole doublets.

This work is supported by the Start-up funds of Fudan University (Shanghai, People’s Republic of China) and the Thousand-Youth-Talent program of People’s Republic of China.

- [1] Z.-C. Gu and X.-G. Wen, Tensor-entanglement-filtering renormalization approach and symmetry-protected topological order, *Phys. Rev. B* **80**, 155131 (2009).
- [2] F. Pollmann, E. Berg, A. M. Turner, and M. Oshikawa, Symmetry protection of topological phases in one-dimensional quantum spin systems, *Phys. Rev. B* **85**, 075125 (2012).
- [3] T. Senthil, Symmetry-protected topological phases of quantum matter, *Annu. Rev. Condens. Matter Phys.* **6**, 299 (2015).
- [4] M. Z. Hasan and C. L. Kane, *Colloquium*: Topological insulators, *Rev. Mod. Phys.* **82**, 3045 (2010).
- [5] X.-L. Qi and S.-C. Zhang, Topological insulators and superconductors, *Rev. Mod. Phys.* **83**, 1057 (2011).
- [6] X.-G. Wen, *Quantum Field Theory of Many-body Systems: From the Origin of Sound to an Origin of Light and Electrons (Oxford Graduate Texts)*, reissue ed. (Oxford University Press, New York, NY, 2007).
- [7] A. Mesaros and Y. Ran, Classification of symmetry enriched topological phases with exactly solvable models, *Phys. Rev. B* **87**, 155115 (2013).
- [8] A. M. Essin and M. Hermele, Classifying fractionalization: Symmetry classification of gapped Z_2 spin liquids in two dimensions, *Phys. Rev. B* **87**, 104406 (2013).
- [9] Y.-M. Lu and A. Vishwanath, Classification and properties of symmetry-enriched topological phases: Chern-simons approach with applications to Z_2 spin liquids, *Phys. Rev. B* **93**, 155121 (2016).
- [10] Y.-P. Huang, G. Chen, and M. Hermele, Quantum Spin Ices and Topological Phases from Dipolar-Octupolar Doublets on the Pyrochlore Lattice, *Phys. Rev. Lett.* **112**, 167203 (2014).
- [11] Y.-D. Li, X. Wang, and G. Chen, Anisotropic spin model of strong spin-orbit-coupled triangular antiferromagnets, *Phys. Rev. B* **94**, 035107 (2016).
- [12] Y.-D. Li, X. Wang, and G. Chen, Hidden multipolar orders of dipole-octupole doublets on a triangular lattice, *Phys. Rev. B* **94**, 201114 (2016).
- [13] We here adopt the definition of the U(1) topological order in Ref. [21]. The concept is more general than the fully gapped intrinsic topological orders that are described by topological quantum field theory.
- [14] R. Sibille, E. Lhotel, V. Pomjakushin, C. Baines, T. Fennell, and M. Kenzelmann, Candidate Quantum Spin Liquid in the Ce^{3+} Pyrochlore Stannate $Ce_2Sn_2O_7$, *Phys. Rev. Lett.* **115**, 097202 (2015).
- [15] G. Chen and L. Balents, Spin-orbit effects in $Na_4Ir_3O_8$: A hyper-kagome lattice antiferromagnet, *Phys. Rev. B* **78**, 094403 (2008).
- [16] G. Jackeli and G. Khaliullin, Mott Insulators in the Strong Spin-Orbit Coupling Limit: From Heisenberg to a Quantum Compass and Kitaev Models, *Phys. Rev. Lett.* **102**, 017205 (2009).
- [17] G. Chen, R. Pereira, and L. Balents, Exotic phases induced by strong spin-orbit coupling in ordered double perovskites, *Phys. Rev. B* **82**, 174440 (2010).
- [18] W. Witczak-Krempa, G. Chen, Y. B. Kim, and L. Balents, Correlated quantum phenomena in the strong spin-orbit regime, *Annu. Rev. Condens. Matter Phys.* **5**, 57 (2014).
- [19] G. Khaliullin, Orbital Order and Fluctuations in Mott Insulators, *Prog. Theor. Phys. Supplement* **160**, 155 (2005).
- [20] G. Chen and L. Balents, Spin-orbit coupling in d^2 ordered double perovskites, *Phys. Rev. B* **84**, 094420 (2011).
- [21] M. Hermele, M. P. A. Fisher, and L. Balents, Pyrochlore photons: The U(1) spin liquid in a $S=1/2$ three-dimensional frustrated magnet, *Phys. Rev. B* **69**, 064404 (2004).
- [22] D. A. Huse, W. Krauth, R. Moessner, and S. L. Sondhi, Coulomb and Liquid Dimer Models in Three Dimensions, *Phys. Rev. Lett.* **91**, 167004 (2003).
- [23] L. Savary and L. Balents, Coulombic Quantum Liquids in Spin-1/2 Pyrochlores, *Phys. Rev. Lett.* **108**, 037202 (2012).
- [24] S. Lee, S. Onoda, and L. Balents, Generic quantum spin ice, *Phys. Rev. B* **86**, 104412 (2012).
- [25] Z. Hao, A. G. R. Day, and M. J. P. Gingras, Bosonic many-body theory of quantum spin ice, *Phys. Rev. B* **90**, 214430 (2014).
- [26] O. Petrova, R. Moessner, and S. L. Sondhi, Hydrogenic states of monopoles in diluted quantum spin ice, *Phys. Rev. B* **92**, 100401 (2015).
- [27] L. Savary, X. Wang, H.-Y. Kee, Y. Kim, Y. Yu, and G. Chen, Quantum Spin Ice on the Breathing Pyrochlore Lattice, *Phys. Rev. B* **94**, 075146 (2016).
- [28] N. Shannon, O. Sikora, F. Pollmann, K. Penc, and P. Fulde, Quantum Ice: A Quantum Monte Carlo Study, *Phys. Rev. Lett.* **108**, 067204 (2012).
- [29] G. Chen, “Magnetic monopole” condensation of the pyrochlore ice U(1) quantum spin liquid: Application to $Pr_2Ir_2O_7$ and $Yb_2Ti_2O_7$, *Phys. Rev. B* **94**, 205107 (2016).
- [30] O. Benton, O. Sikora, and N. Shannon, Seeing the light: Experimental signatures of emergent electromagnetism in a quantum spin ice, *Phys. Rev. B* **86**, 075154 (2012).
- [31] M. J. P. Gingras and P. A. McClarty, Quantum spin ice: A search for gapless quantum spin liquids in pyrochlore magnets, *Rep. Prog. Phys.* **77**, 056501 (2014).
- [32] See Supplemental Material at <http://link.aps.org/supplemental/10.1103/PhysRevB.95.041106> for detailed analysis of the model.
- [33] Brillouin zone, adapted from Wikipedia, https://en.wikipedia.org/wiki/Brillouin_zone.
- [34] M. A. Levin and X.-G. Wen, String-net condensation: A physical mechanism for topological phases, *Phys. Rev. B* **71**, 045110 (2005).
- [35] V. K. Anand, A. K. Bera, J. Xu, T. Herrmannsdörfer, C. Ritter, and B. Lake, Observation of long-range magnetic ordering in pyrochlore $Nd_2Hf_2O_7$: A neutron diffraction study, *Phys. Rev. B* **92**, 184418 (2015).
- [36] E. Lhotel, S. Petit, S. Guitteny, O. Florea, M. Ciomaga Hatnean, C. Colin, E. Ressouche, M. R. Lees, and G. Balakrishnan, Fluctuations and all-in all-out Ordering in Dipole-Octupole $Nd_2Zr_2O_7$, *Phys. Rev. Lett.* **115**, 197202 (2015).
- [37] A. Bertin, P. D. de Réotier, B. Fåk, C. Marin, A. Yaouanc, A. Forget, D. Sheptyakov, B. Frick, C. Ritter, A. Amato, C. Baines, and P. J. C. King, $Nd_2Sn_2O_7$: An all-in all-out pyrochlore magnet with no divergence-free field and anomalously slow paramagnetic spin dynamics, *Phys. Rev. B* **92**, 144423 (2015).
- [38] J. Xu, V. K. Anand, A. K. Bera, M. Frontzek, D. L. Abernathy, N. Casati, K. Siemensmeyer, and B. Lake, Magnetic structure and crystal-field states of the pyrochlore antiferromagnet $Nd_2Zr_2O_7$, *Phys. Rev. B* **92**, 224430 (2015).
- [39] M. Ciomaga Hatnean, M. R. Lees, O. A. Petrenko, D. S. Keeble, G. Balakrishnan, M. J. Gutmann, V. V. Klekovkina,

- and B. Z. Malkin, Structural and magnetic investigations of single-crystalline neodymium zirconate pyrochlore $\text{Nd}_2\text{Zr}_2\text{O}_7$, *Phys. Rev. B* **91**, 174416 (2015).
- [40] S. Petit, E. Lhotel, B. Canals, M. Ciomaga Hatnean, J. Ollivier, H. Mutka, E. Ressouche, A. R. Wildes, M. R. Lees, and G. Balakrishnan, Observation of magnetic fragmentation in spin ice, *Nat. Phys.* **12**, 746 (2016).
- [41] J. Lago, I. Živković, B. Z. Malkin, J. Rodriguez Fernandez, P. Ghigna, P. Dalmas de Réotier, A. Yaouanc, and T. Rojo, CdEr_2Se_4 : A New Erbium Spin Ice System in a Spinel Structure, *Phys. Rev. Lett.* **104**, 247203 (2010).
- [42] S. Pokrzywnicki, Analysis of the magnetic susceptibility of CdYb_2S_4 spinel by means of the crystal field method, *Phys. Stat. Sol. (b)* **71**, K111 (1975).